Journal of the Nigerian Association of Mathematical Physics
***Volume* 22 (November, 2012), pp 111 – 118**
© J. of NAMP

Surface Characterisation of Copper Oxide Thin Films Prepared By RF Magnetron Sputtering

Darma T.H. and Taura L.S.

Department of Physics,
Bayero University, P.M.B. 3011 Kano-Nigeria

Abstract

Surface properties of copper oxide thin films prepared at various deposition conditions on glass and silicon wafer substrates by rf magnetron sputtering using copper target in an argon-oxygen gas mixtures were investigated. The films were characterized by Scanning electron microscopy, Atomic force microscopy, X-ray photoelectron spectroscopy, X-ray diffraction studies, Fourier transform infra-red spectroscopy, and optical transmission and reflection measurement. The films were found to be predominantly of the Cu_2O phase as indicated by X-ray diffraction studies and FT-IR. The morphology studies reveal films with dense and columnar structure. Surface roughness of 2.1nm – 10.2nm was observed for the films. Optical transmission greater than 60% was observed in the visible region. The presence of CuO phase was confirmed by the XPS.

Keywords: copper oxides, surface energy, contact angle, rf magnetron sputtering.

.

1.0 Introduction

The two major oxides of copper are cuprous oxide (Cu_2O), and cupric oxide (CuO). Cuprous oxide (Cu_2O), a known p-type semiconductor with a band gap of 2.0eV is shiny and has a yellow-orange appearance. It is cubic in structure and is mostly investigated on its potential viability as a photovoltaic material. It has high absorption coefficient in the visible range (0.35 – 0.8μm) and reasonably good electrical properties as a solar cell with theoretical achievable efficiency up to 13% [1]. Photocurrent of up to 17.6mAcm^{-2} has been reported for Cu_2O cells [2]. Cuprous oxide is shown to have potential as a material for electrochromism [3], solar light modulation [4], window coatings for solar control [5], and material for photocatalysis to achieve solar light induced splitting of water in photo-electrochemical (PEC) cells [6].

CuO with a band gap of 1.3eV has good photoconductive and photo-thermal properties and is the basis of several high-T_c superconductors. CuO has also been reported as an electrode in Li-ion batteries [7]. CuO and Cu_2O have also been synthesized for gas sensing applications [8].

Various methods of thin film deposition have been employed for the preparation of copper oxides which includes; electrodeposition [9], chemical vapour deposition [10], sol-gel dip technique [11], chemical bath deposition [12], reactive magnetron sputtering [13,14,15], and thermal oxidation [16] among others.

Most of the reported methods of growing Cu_2O results in a combined growth of the copper I oxide (Cu_2O) and copper II oxide (CuO). The contamination from CuO is often a serious problem in the growth of Cu_2O films. Phase purity and stability of Cu_2O has been an important issue affecting its application in solar cells and other devices.

The physical, electrical, and optical properties of copper oxides have been widely investigated in the literature both theoretically and experimentally. Few reports are also available on surface properties such as surface energy based on single phase CuO [17] and mixed oxides [13], both prepared by magnetron sputtering, and density functional theory method [18]. The aim of this work is to investigate the surface properties of predominantly cuprous oxide thin films prepared by rf magnetron sputtering at different deposition conditions.

*Corresponding author: ***Darma T. H.,*** E-mail: thdarma@yahoo.co.uk , Tel. +234 8107596053

Theoretical background

Contact angle θ, is the angle formed by a liquid at the three phase boundary where a liquid, gas and solid intersect. Precise characterisation of material surfaces and liquids plays a vital role in development of new, better performing products with improved qualities. Measurement of contact angles and surface/interfacial tensions provides a better understanding of the interactions between solids and liquids or liquids/liquids. These interactions play a key role in understanding adhesion, material wettability, biocompatibility, lubricity of solid surfaces as well as wetting, washability, spreading and adsorption of liquids. θ as a quantitative measure of the wetting of a solid by a liquid, can also be used as a quality control measure in surface treatments and surface cleanliness.

Contact angle and surface/interfacial tension measurements provide the information required for the development and modification of liquid and solid surfaces. One of the methods used in the determination of the static or dynamic contact angles, absorption and surface/interfacial tensions of a liquid is the pendant drop method. In the pendant drop method, the surface/interfacial tension is determined by analysing the shape of the drop of liquid hanging from the tip of a syringe. The shape of the drop is controlled by the three forces of interfacial tension.

The drop profile is extracted from its stored image with sub-pixel accuracy. This profile is then curve fitted to the Young – Laplace equation. The entire fitted curve may then be used to calculate contact angle and or surface tension [19].

Contact angle measurement is used to relate the key thermodynamic parameters of a surface through the Young equation given by

$$\gamma_{lv} \cos\theta = \gamma_{sv} - \gamma_{sl} \qquad (1)$$

where γ_{lv}, γ_{sv}, and γ_{sl} are the liquid-vapour, solid-vapour, and solid-liquid interface energies respectively. The surface energy components provide necessary information for understanding the factors that underpin the durability and resistance of the films to environmental changes like water and fog condensation. The first two terms in Young's equation can be determined experimentally, while the remaining terms are estimated based on theoretical considerations classified into either microscopic or macroscopic approaches for determining the surface energy. In the microscopic theories, the total surface energy can be expressed as;

$$\gamma = \gamma^p + \gamma^d. \qquad (2)$$

where γ^p is the polar component of the surface energy and γ^d is the dispersive component of the surface energy [19]. The microscopic theories of surface energy can also be separated into two approaches depending on the type of combining rule used to determine the surface energy from its dispersive and polar components. These approaches are the geometric mean proposed by Fowkes, and Owens and Wendt. The second approach is the Lifshitz-van der Waals acid-base approach developed by Van Oss et-al [19] given as

$$\gamma_s = \gamma_s^{LW} + \gamma_s^{AB}, \qquad \text{where} \gamma_s^{AB} = 2(\gamma_s^{+}\gamma_s^{-})^{1/2} \qquad (3)$$

where $\gamma_s^{+} and \gamma_s^{-}$ are the acid and base components of the Lewis acid-base interaction terms. The calculation of γ_s involve carrying out contact angle measurements on three liquids. Two of which are polar liquids and one of which is dispersive liquid. A similar approach to the Owens-Wendt approach is then used to solve the resulting equation. The three liquids usually used are water, ethylene glycol, and diiodomethane [19].

2.0 Experimental investigation

The experiment was performed with a cryo-pumped vacuum chamber (CVC) rf magnetron sputtering unit AST304. Prior to deposition, the chamber was evacuated to a base pressure of 10^{-6} T. Glass slides and silicon wafer which were cleaned ultrasonically with iso-propanol and then washed with de-ionised water were used as substrates. High purity argon and oxygen were used as the sputtering and reactive gases. The target was pre-sputtered in pure Argon atmosphere for 3 minutes to remove oxide layers if any on the surface of the target. The deposition conditions are given in Table 1.

Table 1. Film Deposition Conditions

Target:	Copper
Substrate:	Glass, Silicon wafer
Deposition time:	5 min
Forward power:	200, 300, 400, 500, & 600W
Reflected power:	<1W
Argon flow rate:	50 sccm
Oxygen flow rates:	2, 3, 4, 6 sccm
Chamber pressure:	3.0, 4.0, 6.0 mTorr
Substrate temperature:	room temperature

3.0 Results and discussion

SEM

Scanning electron micrographs of the films prepared at forward power of 200W – 600W with different combinations of oxygen flow rate and deposition pressure have dense columnar structures but with a little rough surfaces. The surface roughness was seen to increase with increasing power. The SEM micrographs of the films prepared at 400 – 600W power are shown in Fig. 1.

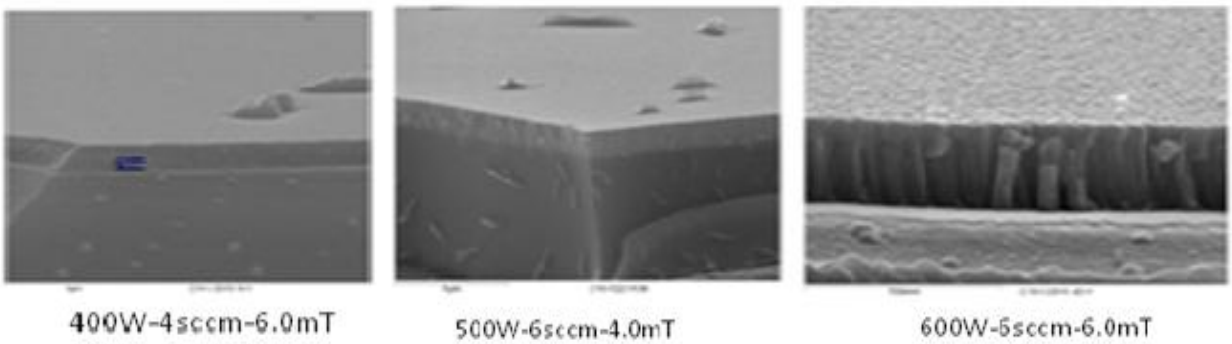

Fig. 1 Cross-sectional view of scanning electron micrographs of films prepared at different deposition conditions

AFM

Atomic force topography of film prepared at 500W power, 6.0sccm oxygen flow rate, and 4.0mT pressure is shown in Fig. 2. The film has a surface roughness of 4.6nm.

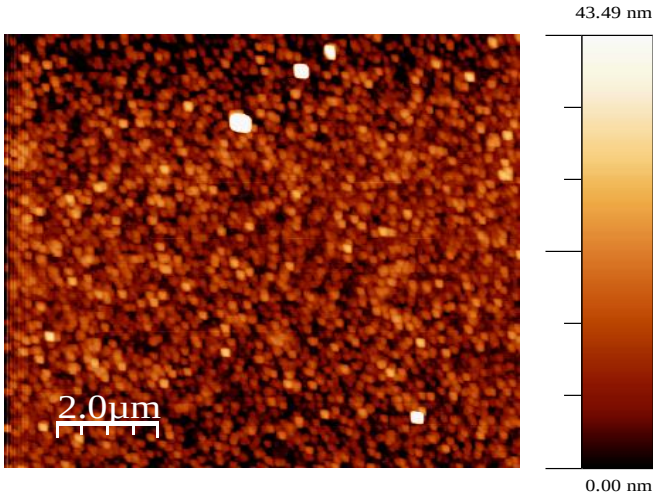

Fig. 2 AFM topography of film prepared at 500W power, 6sccm oxygen flow and 4.0mT pressure XRD

The X-ray diffraction spectra of films prepared at different deposition conditions are shown in Fig 3. The film prepared at 400W power, 4sccm oxygen flow rate, and 6.0mT pressure depicts a strong broad peak at $2\theta = 36.9^o$ (d= 2.431Å) corresponding to the (111) plane of Cu_2O phase which is stable due to small grain size, and a weak peak at $2\theta = 42.8^o$ (d= 2.112Å) corresponding to the (200) plane of the cubic Cu_2O phase. The film prepared at 500W power using 6sccm oxygen flow rate and 4.0mT pressure depicts a spectra with strong peak at $2\theta = 36.2^o$ (d= 2.483Å) corresponding to the (111) plane of cubic Cu_2O phase, and weak peaks at $2\theta = 38.3^o$ (d= 2.350Å), $2\theta = 51.8^o$ (d= 1.764Å), and $2\theta = 71.3^o$ (d= 1.322Å) which can be attributed to the (111), (112), and $(\bar{3}12)$ planes of the monoclinic CuO phase respectively, and at $2\theta = 43.2^o$ (d= 2.093Å) corresponding to the (111) plane of un-oxidised Cu.

The spectra of the film prepared at 600W power, 6sccm oxygen flow rate and 6.0mT pressure, is also polycrystalline in nature. The spectra show strong peaks at $2\theta = 36.9^o$ (d= 2.434Å) and $2\theta = 42.9^o$ (d= 2.102Å) which can be attributed to the (111) and (200) planes of the cubic Cu_2O phase, a medium peak at $2\theta = 38.4^o$ (d= 2.344Å) which can be attributed to the (111) plane of the monoclinic CuO phase, and a weak peak at $2\theta = 51.6^o$ (d= 1.770Å) which can be attributed to the (112) plane of CuO phase as well.

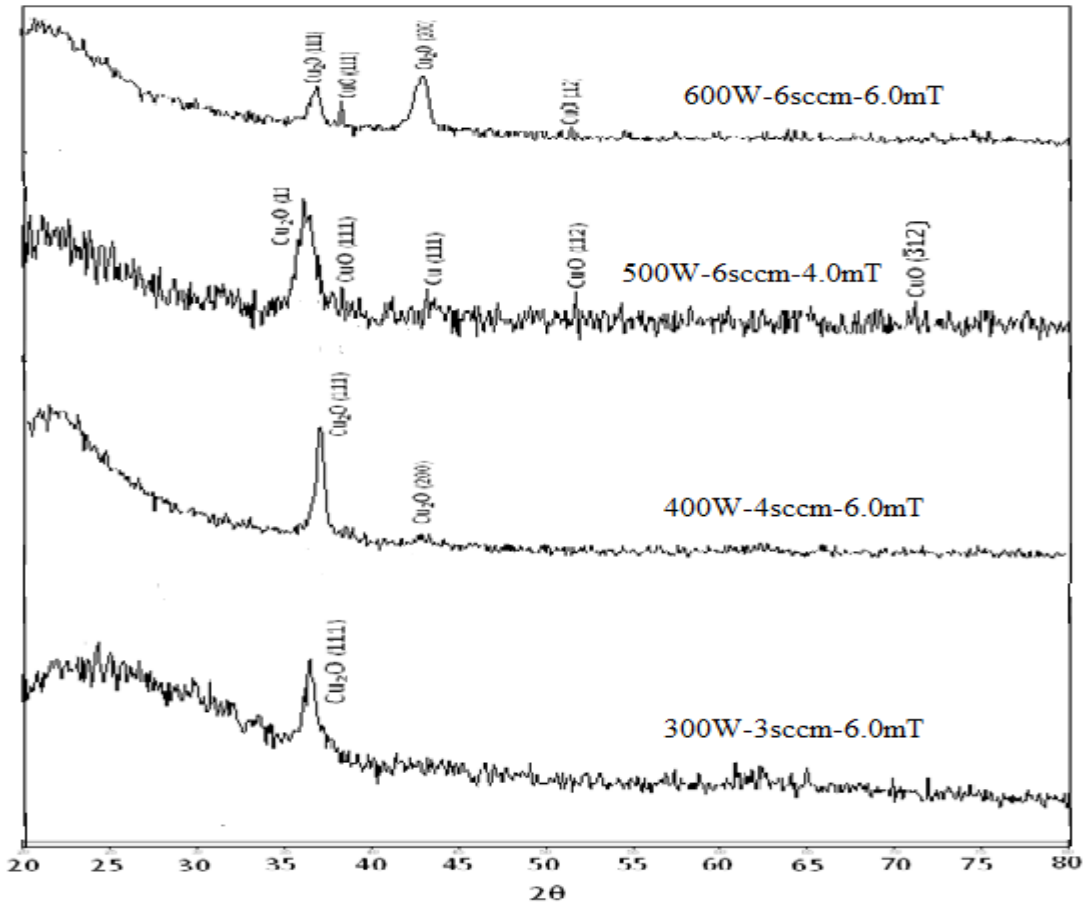

Fig. 3. X-ray diffraction spectra of films prepared at different deposition conditions

XPS

Normalized spectra's based on the intensity of Cu 2p peaks of films prepared at different deposition conditions are shown in Fig. 4.

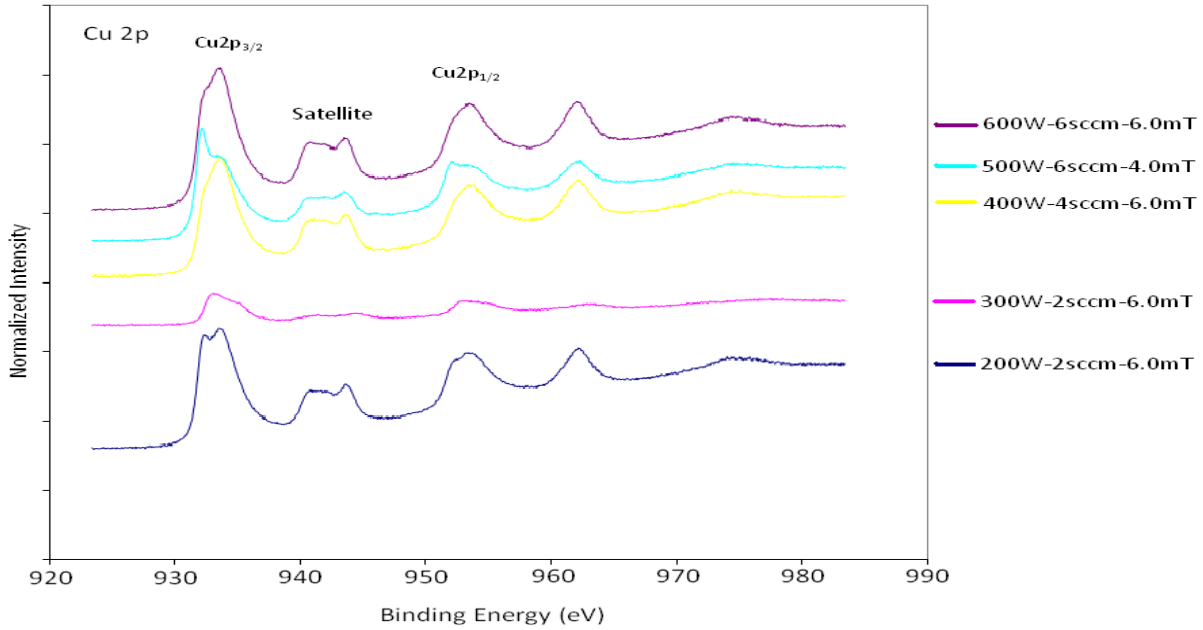

Fig. 4. Normalized spectra's based on the intensity of Cu 2p peaks. The two sublevels of the Cu 2p peak along with the satellite structure in the films are shown

The broad Cu $2p_{3/2}$ deconvolution for the film prepared at 400W power, 4sccm oxygen flow, and 6.0mT pressure is shown in Fig. 5. The two peaks are positioned at 932.5eV corresponding to Cu_2O [20], and 933.6eV corresponding to CuO [20,21] with a FWHM of 1.1 and 2.9eV respectively. Ghodselahi et-al [22] has reported a FWHM of 2.8eV attributed to CuO. The FWHM is less than the reported values of 1.9eV and 3.4eV for the respective oxides. The satellite to main peak ratio (I_s/I_m) is 0.43. The main peak of the O 1s spectra is located at 529.5eV with a FWHM of 0.8eV, while the second component is located at 531.1eV with a FWHM of 1.6eV. The main peak to satellite area ratio is 1.6.

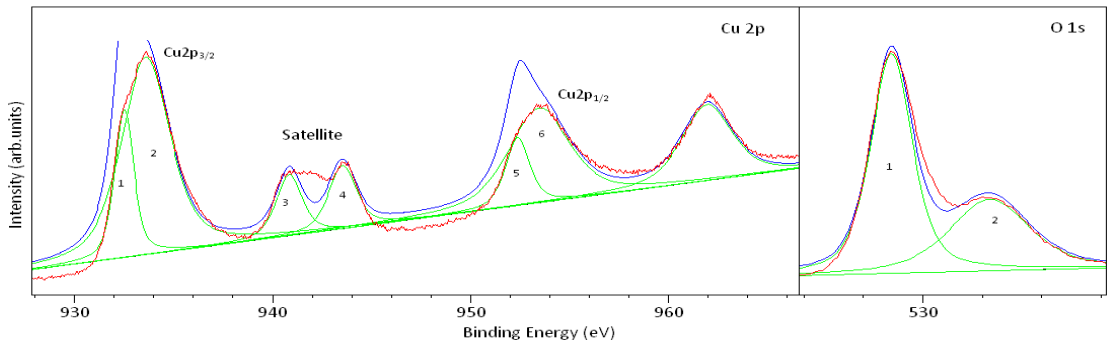

Fig 5- Fitted profile of the Cu 2p and O 1s peaks for the film prepared at 400W power, 4sccm oxygen flow rate, and 6.0mT pressure on glass substrate

Table 2 shows the binding energies, full-width at half maximum of Cu $2p_{3/2}$ and O 1s core level regions of the oxide films prepared at different deposition conditions.

Table 2 XPS binding energies (BE) and full-width at half-maximum (β) of oxide films in the deconvoluted Cu $2p_{3/2}$ and O 1s core level regions

RF Power (W)	Power Density (W/cm^2)	O_2 Flow Rate (sccm)	Pressure (mT)	Binding Energy (BE)/FWHM (β)							
				Cu $2p_{3/2}$				O 1s			
				BE (1)	β	BE (2)	β	BE (Main)	β	BE Satellite)	β
200	0.6	2	6	932.4	1.1	933.6	3.1	529.6	0.9	531.1	1.6
300	0.9	2	6	932.5	1.6	934.4	1.5	529.7	1.3	531.5	1.5
400	1.2	4	6	932.5	1.1	933.6	2.9	529.5	0.8	531.1	1.6
500	1.5	6	4	932.2	1.1	933.7	2.8	529.6	1.2	531.1	1.5
600	1.9	6	6	932.5	1.5	933.6	2.9	529.4	0.9	531.2	1.4

FT-IR

The FT-IR characterisation of films prepared at 300W, 400W, 500W, and 600W and different oxygen flow rates and deposition pressures on Silicon wafer show single absorption band characteristics of the Cu-O vibration in Cu_2O. A strong absorption band at $611cm^{-1}$ was observed for the Si wafer substrate in agreement with the report by Balamurugan and Mehta [1]. The absorption bands observed at $615cm^{-1}$ are in close agreement with reports [16,23], for vibrations of Cu-O in Cu_2O. No absorption band associated with Cu-O vibration in CuO was observed as shown typically in Fig. 6 for the film prepared at 500W power.

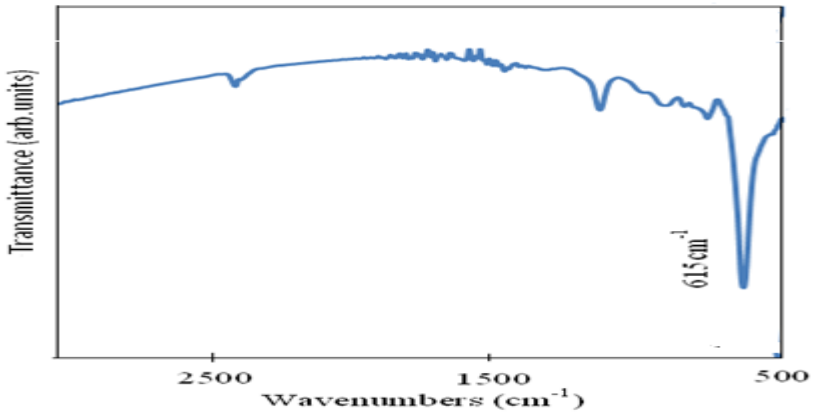

Fig. 6 FT-IR spectra of film prepared at 500W power, 6.0sccmoxygen flow rate and 4.0mT pressure

Contact angle and Surface energy

The contact angle was found to depend on the nature of the probe liquids. The highest contact angle was obtained with water, the most polar liquid, while the lowest contact angle was obtained with diiodomethane, which is the most dispersive liquid. This suggests that the copper oxide films are hydrophobic in nature, which is in agreement with previous report [19]. The hydrophobic nature of the films is important for their potential applications in solar cells or window coatings, since they cannot be easily wet by water.

It is worth noting that, variations in the contact angle with forward power and oxygen flow rates were observed. The contact angle was found to change with changes in forward power and oxygen flow rates as shown in Fig. 7. This is somehow different from the report in [19], which suggest little variation with oxygen flow rates. It is thought that difference in the deposition time (leading to thicker films) and the use of single syringe for each liquid (which reduces possible contamination) contributed to the variations in the contact angle.

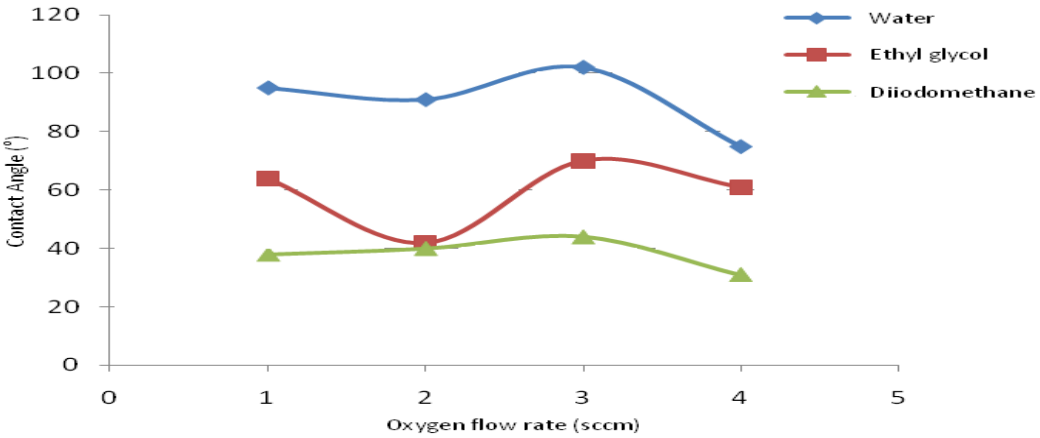

Fig 7. Variation of contact angle with oxygen flow rates for the three liquids at constant forward power of 300W for films prepared on glass substrate

Results from this investigation indicate that both forward power and oxygen flow rates affect the surface energy of the copper oxide films. Table 3 shows the surface energy terms of films prepared at different rf power and oxygen flow rates.

The range of surface energy components in this report is within reported values by Goto et al [17] and Ogwu et al [19]. The surface energy components provide the necessary information for understanding the factors that underpin the durability and resistance of the films to environmental changes like water and fog condensation. The contact angle and surface energy terms reported are indicative of hydrophobic films in agreement with Ogwu et al [19].

Table 3 The Fowkes, Wu, and AB Surface Energy terms in mJ/m^2 for Copper Oxide films compared at different rf Power and 6 sccm oxygen flow

RF Power (W)	O_2 Flow (sccm)	Fowkes γ^{total}	Fowkes γ^{d}	Fowkes γ^{p}	Wu γ^{total}	Wu γ^{d}	Wu γ^{p}	AB γ^{total}	AB γ^{lw}	AB γ^{+}	AB γ^{-}
400	6	38.97	38.94	0.03	39.58	38.36	1.22	37.29	37.47	0.45	0.21
500	6	32.34	26.92	5.41	38.52	32.22	6.30	22.05	35.70	1.42	4.80
600	6	26.27	24.73	1.54	30.38	26.88	3.51	26.19	25.00	0.46	1.29

Optical transmission

The transmission and reflection plot for the films prepared at 400W power, 4sccm oxygen flow rate, and 6.0mT pressure depicts a transmission that Is above 60% as shown in Fig. 8. The film has a yellow colouration which changes with increasing pressure to grey. The reflectance spectrum was seen to have a minimum. According to Derin and Kantarli [24] who investigated thermally oxidised copper films, the reflectance spectrum is a reliable indication of the oxide composition in the film. The colour change arises from film thickness with the reflectance drop passing a minimum at wavelength between 400nm – 600nm in the reflectance spectrum of the Cu_2O – Cu system. If the oxide films were CuO, the reflectance value would be zero for all wavelengths in the visible and therefore all samples of different thickness would be black.

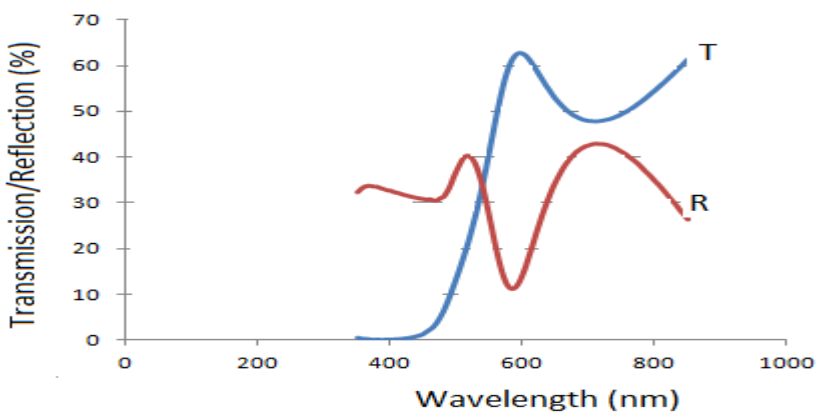

Fig. 8. Optical transmission and reflection of film prepared at 400W power, 4sccm oxygen flow rate and 6.0mT pressure

Conclusion:

Copper oxide films of predominantly Cu_2O phase at the surface, has been prepared at various deposition conditions. The highest contact angle was obtained with water, the most polar liquid, while the lowest contact angle was obtained with diiodomethane, which is the most dispersive liquid. These suggest that the copper oxide films are hydrophobic in nature, which is in agreement with reports in the literature. A further confirmation of the hydrophobic nature of the copper oxide films is that the predominant term in the surface energy of the copper oxide films is the dispersive term (γ^d) in the Fowkes/Wu approach and the London-van der Waals term (γ^{lw}) term in the VOGG approach which explains the minimal interaction with water and the resulting high contact angle, while the polar component (γ^p) values of the surface energy of the prepared oxide films are very small compared to the dispersive component.

References:

[1]. B. Balamurugan and B.R. Mehta; Thin Solid Films, 396 (2001) 90 – 96

[2]. L.C. Olsen, F.W. Addis, and W. Miller; Solar Cells**, 7** (1982) 247 – 279

[3]. R. Neskovska, M. Ristova, J. Velevska, and M. Ristov; Thin Solid Films 515 (2007) 4717–4721

[4]. M. Ristov, Gj. Sinadinovski, and I. Grozdanov; Thin Solid Films, 123**,** 1 (1985) 63 – 67

[5]. G. Correa and R. Almanza; Solar Energy, 76 (2004) 111 – 115

[6]. Lei Huang, Feng Peng, Hao Yu, Hongjuan Wang; Solid State Sciences, 11 (2009) 129 – 138

[7]. H. Zhang and Z. Cui; Materials Research Bulletin 43 (2008) 1583–1589

[8]. D. Barreca, E. Comini, A. Gasparotto, C. Maccato, C. Sada, G. Sberveglieri , E. Tondello; Sensors and Actuators B, 141 (2009) 270 – 275

[9]. T. Mahalingama, J.S.P. Chitraa, J.P. Chub, P.J. Sebastian; Material Letters 58 (2004) 1802 – 1807

[10]. Toshiro Maruyama; Solar Energy Materials and Solar Cells 56 (1998) 85 – 92

[11]. Sekhar C. Ray; Solar Energy Materials and Solar Cells, 68 (2001) 307 – 312

[12]. (Longcheng Wang and Meng Tao; *Electrochemical and Solid-State Letters*,0 **(**9) H248-H250 (2007))

[13]. A A Ogwu, E Bouquerel, O Ademosu, S Moh, E Crossan and F Placido; Journal of Physics D: Applied Physics 38 (2005) 266

[14]. K. Akimoto, S. Ishizuka, M. Yanagita, Y. Nawa, Goutam K. Paul, T. Sakurai; Solar Energy 80 (2006) 715 – 722

[15]. E.M. Alkoy and P.J. Kelly; Vacuum 79 (2005) 221 – 230

[16]. G. Papadimitropoulos, N. Vourdas, V. Em. Vamvakas, D. Davazoglou; Thin Solid Films, 515 (2006) 2428 – 2432

[17]. Masahiro Goto, Akira Kasahara, Masahiro Tosa; Journal of Applied Physics, Vol. 94, 3 (2003)

[18]. A. Soon, M. Todorova, B. Delley, and Catherine Stampfl; Physical Review B 75, 125420 (2007)

[19]. A.A. Ogwu, E. Bouquerel, O. Ademosu, S. Moh, E. Crossan, and F. Placido; Acta Materiala 53 (2005) 5151 – 5159

[20]. J. Morales; Thin Solid Films 474 (2005) 133 – 140

[21]. M.F. Al-Kuhaili; Vacuum 82 (2008) 623 – 629

[22]. T. Ghodselahi, M.A. Vesaghi, A. Shafiekhani, A. Baghizadeh, M. Lameii; Applied Surface Science 355 (2008) 2730 – 2734

[23]. D.S.C. Halin, I. A. Talib, , M. A. A. Hamid, A. R. Daud; Solid State Science and Technology, Vol. 16, No 1 (2008) 232 – 237

[24]. H. Derin and K. Kantarli; Applied Physics A 75, (2002) 391 – 395